Independent Component Analysis for sleep-spindles detection using an Extended Infomax Algorithm and Fixed-point Algorithm.

Roman Rosipal, Georg Dorffner

Institute of Measurement Science, Slovak Academy of Sciences

University of Vienna,
Department of Medical Cybernetics and Artificial Intelligence
&
Austrian Research Institute for Artificial Intelligence

June 1998

A shorter version of this technical report will appear in:
Proceedings of SCANN, November 1998.

Independent Component Analysis for sleep-spindles detection using an Extended Infomax Algorithm and Fixed-point Algorithm.

Roman Rosipal
Institute of Measurement Science
Slovak Academy of Sciences
Dúbravská cesta 9, 842 19 Bratislava, Slovakia
e-mail: rosipal@neuro.savba.sk

Georg Dorffner
Dept. of Medical Cybernetics and Artificial Intelligence
University of Vienna
Freyung 6/2, A-1010 Vienna, Austria
and
Austrian Research Institute for Artificial Intelligence
Schottengasse 3, A-1010 Vienna, Austria
e-mail: georg@ai.univie.ac.at

Abstract

We investigated the possibility to use the Independent Component Analysis (ICA) as a method for preprocessing the sleep EEG data with the aim to improve detection of sleep spindles - specific phenomena of sleep EEG recordings prevailingly occurring during the stage 2 of the sleep. We projected the strengths of individual Independent Components (ICs) onto the scalp sensors to detect potential spatial localization of sleep-spindles sources. We used two different algorithms for ICs separation with aim to compare the fitness of the algorithms in sleep-spindle detection problem.

1 Introduction

Sleep spindles are specific phenomena of electroencephalograms (EEG), (i.e. recordings of the electrical activity of the brain) during sleep. They may by defined as a group of rather broad frequency (11.5 - 15 Hz) oscillations with evidence for variability and heterogeneity [15]. Occurrence of sleep spindles is one criterion of standard criteria of sleep stages classification defined 30 years ago by Rechtschaffen and Kales [12]. Thus the correct automated detection of spindles can increase the accuracy of sleep stage classification.

The visual analysis of sleep spindles is highly time-consuming and difficult in the case of multi-channels recordings. In [13] automatic sleep spindle detection algorithm was proposed. Criteria based on definition of frequency, amplitude and duration properties of human sleep spindles were used on raw EEG recordings. The another heuristic criteria were used to distinguish among muscle artifacts, fast alpha activity and sleep spindles. Although the results using one EEG channel are promising the problem of multi-channel sleep spindle detection caused by time-delays between occurrence of spindles in different channels is still open.

In this paper we used a Independent Component Analysis (ICA) to separate a sleep spindle activity from multi-channels EEG recordings. The method is based on the assumption that the EEG measured on the human scalp is a linear mixture of anatomically and physiologically separate processes of the brain. The results of using ICA for auditory event-related potentials detection [10], extraction of ocular artifacts from EEG [14] and removing artifacts from EEG [7] encourage us to use ICA in our case. The separated 'sleep spindle' signal we used for successive sleep spindle classification.

In our study we used two different ICA algorithms. The first one is an extended version of the *infomax* algorithm [2]. The modification based on learning rule derived by Girolami [4] gets over the incapability of the original algorithm to separate the mixtures of sub-Gausssian sources. The better convergence property is achieved by using the 'natural' gradient proposed by Amari et al. [1] or 'relative' gradient proposed by Cardoso and Laheld [3]. The second, very fast *fixed-point* algorithm based on maximising new approximations of differential entropy was derived by [5, 6]. Both algorithms were recently used for separation of the EEG sources [9, 14].

2 Independent component analysis (ICA)

The problem of ICA can be simply formulated as finding a set of statistically independent signal sources from their linear mixture. Usually in ICA we observe m scalar random variables $x_1, x_2, ..., x_m$ which are assumed to be linear combinations of n unknown independent components (ICs) $s_1, s_2, ..., s_n$. In matrix notation we can write

$$\mathbf{x} = \mathbf{A}\mathbf{s},$$

where $\mathbf{A}$ is an unknown $m \times n$ mixing matrix (here we will assume that $n \leq m$). The goal of the ICA is then to estimate the inverse of the matrix $\mathbf{A}$ and the ICs using only observations $\mathbf{x}$.

Several algorithms based on information theory were proposed (see review [8]). Nadal and Parga in [11] showed that maximum of the mutual information between the input and output of the neural unit is achieved in the case of the factorial coding of the output distributions. This means the independence of the outputs. Bell and Sejnowski [2] proposed *infomax* algorithm for estimation of the inverse of the matrix $\mathbf{A}$ based on maximisation of the mutual information between the input and output. They assumed neural-like structure with an input vector $\mathbf{x}$, a weight matrix $\mathbf{W}$ (estimation of the inverse of the matrix $\mathbf{A}$) and a monotonically transformed output vector $\mathbf{y} = G(\mathbf{u})$ where $\mathbf{u} = \mathbf{W}\mathbf{x}$. Thus the components of the output vector $\mathbf{y}$ represent the estimated source signals. Next, they showed that in the case of invertible deterministic mapping $G(.)$, the mutual information between input and output can be maximised by maximising the entropy of the output alone and it means minimising the mutual information between the output components. Using the gradient ascent of entropy of the output vector $\mathbf{y}$ (with density $f(.)$)

$$H(\mathbf{y}) = -\int_{-\infty}^{+\infty} f(\mathbf{y}) \log f(\mathbf{y}) d\mathbf{y}$$

with respect to matrix $\mathbf{W}$ they derived the iterative algorithm to update the matrix $\mathbf{W}$:

$$\Delta\mathbf{W} \propto [(\mathbf{W}^T)^{-1} - \psi\mathbf{x}^T]$$

where

$$\psi_i(u_i) = \frac{G_i''}{G_i'}(u_i).$$

To improve the convergence rate the 'natural' gradient was proposed [1], or equivalently the relative gradient [3]:

$$\Delta \mathbf{W} \propto [\mathbf{I} - \psi \mathbf{x}^T]\mathbf{W}.$$

Unfortunately, the proposed algorithm fails in the case of separation of sources with negative kurtosis distributions, i.e. sources with a more flat distribution than Gaussian. The extended *infomax*[1] algorithm which allows separation of mixtures of super-Gaussian (i.e. with positive kurtosis) and sub-Gaussian (i.e. with negative kurtosis) sources was proposed by Girolami [4]. The extension is based on using a negentropy (i.e. $J(p_u) = H(p_g) - H(p_u)$, where $H(p_u)$ is entropy of the data density $\mathbf{u}$ and $H(p_g)$ is a entropy of a Gaussian density which has equal mean and covariance) as a projection pursuit index. The final version of the extended infomax using 'natural' gradient is:

$$\Delta \mathbf{W} \propto [\mathbf{I} - \mathbf{K}tanh(\mathbf{u})\mathbf{u}^T - \mathbf{u}\mathbf{u}^T]\mathbf{W} \ ,$$

where $\mathbf{K}$ is a diagonal matrix with elements $sign(k_4(u_i))$ and $k_4(u_i)$ is the kurtosis of the source estimate u_i. $k_4(u_i)$ equals 1 for super-Gaussian and -1 for sub-Gaussian sources.

The other ICA approach we used in our study was *fixed-point - FastICA*[2] algorithm proposed in [5, 6]. The main idea of the algorithm is based on using a new contrast function

$$J_G(\mathbf{w}) = [E\{G(\mathbf{w}^T\mathbf{x})\} - E\{G(\nu)\}]^2 \ ,$$

as an approximation of the negentropy measure of a zero-mean random variable $\mathbf{x}$. Maximising of the negentropy corresponds to minimising the mutual information. ν is a standardized Gaussian variable and it is assumed that $E(\mathbf{w}^T\mathbf{x})^2 = 1$. Such a contrast function can reflect a different statistical property of the individual sources. For example, using $G(z) = z^4$, J_G becomes simply the kurtosis of $\mathbf{z}$. Maximising $J_G(\mathbf{w})$ leads to finding a vector $\mathbf{w}$ in one step and thus to determine one IC. Decorrelation of $\mathbf{w}_k^T\mathbf{x}$ after kth iteration from previously determined outputs $\mathbf{w}_1^T\mathbf{x}, \mathbf{w}_2^T\mathbf{x}, ..., \mathbf{w}_{(k-1)}^T\mathbf{x}$ allows to estimate ICs one by one [5]. The vectors $\mathbf{w}_1, ..., \mathbf{w}_m$ form the unmixing matrix $\mathbf{W}$ and components of the vector $\mathbf{u} = (u_1, u_2, ..., u_n)^T = \mathbf{W}\mathbf{x}$ are estimated ICs. As $\mathbf{W}$ is not the exact inverse of $\mathbf{A}$, $\mathbf{WA} = \mathbf{PD}$ (where $\mathbf{P}$ is a permutation matrix and $\mathbf{D}$ is a diagonal matrix), separation is unambiguous only up to permutation and scaling of the source signals.

First the data are sphered or whitened. This means that $\mathbf{x}$ is linearly transformed by matrix $\mathbf{S}$ to a new variable with correlations matrix equaling unity. This can be achieved by classical Principal Components Analysis. This will change the total estimated unmixing matrix to $\mathbf{WS}$ instead of $\mathbf{W}$. Next, one vector $\mathbf{w}$ is estimated by an iterative *fixed-point algorithm*:

$$\mathbf{w}^+ = E\{\mathbf{x}g(\mathbf{w}^T\mathbf{x})\} - E\{g'(\mathbf{w}^T\mathbf{x})\}\mathbf{w}$$
$$\mathbf{w}^* = \mathbf{w}^+/\|\mathbf{w}^+\|$$

where g and g' are first and second derivatives of the function G and $\mathbf{w}^*$ is a new estimated value of $\mathbf{w}$. As a concrete choice of non-linearity we chose the function $G = logcosh(x)$. The benefits of several non-linear function G were discussed in [5].

3 Simulated data

We reconstructed the artificial problem to demonstrate the possibility of ICA to separate the signal (s_1), consisted from several consequent sleep spindles, from its random mixture with periodic (s_2) and white noise with Gaussian distribution (s_3) signals.

The source signals (s_1, s_2, s_3), mixed signals (x_1, x_2, x_3) and estimated source signals (u_1, u_2, u_3) and (y_1, y_2, y_3) are presented in Fig.1, Fig.2, Fig.3 and Fig. 4, respectively.

In spite of the fact that sleep spindles are transient events in range of 0.5sec to several seconds, it is clear that ICA separates spindle signal with high accuracy. There is no difference between performance of the extended *fixed-point* (Fig.3) and *infomax* (Fig.4) algorithms. The permutation and scaling of the original sources is easy to notice.

[1] Matlab code is available from http://www.cnl.salk.edu/tewon/ica_cnl.html
[2] Matlab code is available from http://www.cis.hut.fi/projects/ica/fastica/

4 Real data

A 7min recording of 18 channels EEG (Fp1, F8, F4, Fz, F3, F7, T4, C4, Cz, C3, T3, T6, P4, Pz, P3, T5, O2, O1) was used . Electrodes were placed according to the international 10-20 system. The data were digitized with a sampling rate of 102.4 Hz. Two EOG channels didn't contribute to better spindle detection on our data set so we didn't use them in results presented in this report.

The fast *fixed-point* ICA algorithm and extended *infomax* were applied on all 43008 data points (7min). The using the subsequent 5000 (49sec) data points intervals leaded to slightly worse classification results as using total data set. To evaluate efficacy of ICA preprocessing we compared the accuracy of spindles detection using the raw EEG data and the IC data. In [13] a technique for spindle detection from raw EEG was introduced. In our investigations we used a simpler algorithm. The raw EEG and IC were band pass filtered using the spindle-frequency band 11.5 -16 Hz. The filtered data were transformed to the ± 1 range and mean-square amplitude (MSA) was calculated at each data point by sliding window with length 0.5sec (the 0.5sec was defined as minimum of sleep spindle duration [13]). A random 30sec data interval was selected to determine the threshold constant (TC) for MSA. The TC was set up to correctly classify the spindles detected by an experienced electroencephalographer during this time interval. This was done for every EEG channel separately. The optimal TC for all 30sec intervals was unable to determine for several channels due to impossibility to distinguish between the correct classification and false positive classification as is illustrated in Fig.5. Using the TC criterion the spindle was detected if at least 0.25sec was value of MSA greater than TC.

The time delays between the spindles in different channels make the detection problem more complicated. We simply detected a spindle at time point i if the spindle was detected at least in one of the channels. This 'advantage' in the detection procedure can lead to unwanted effect, i.e. by classifying several consequent spindles as one event (this was confirmed in our experiments).

The possibility to use the columns of inverse of the estimated matrix ($\mathbf{W}^{-1}$) as the projection strengths of individual ICs onto the scalp sensors was proposed in [10]. We used the Matlab code[3] for these projections. Two different 50sec data intervals were used. The both intervals were divided into two 25sec segments and the first 10 ICs were computed by *fixed point* algorithm for each segment. Here, we have to say that the 25sec intervals were intentionally selected to seize 'local' distributions of spindles during these intervals. The choice of shorter time intervals is constrained by the convergence of the ICA algorithm. The 'spindle' ICs were settled visually.

5 Results

Fig.6 depicts 8 channels of EEG (Fp1, F8, F4, Fz, C4, C3, P4, Pz) during a random 12sec interval. The sleep spindles detected by electroencephalographer are expressed by marks. The first 10 time aligned ICs computed by *fixed-point* algorithm are shown in Fig.7. The correct locations of spindles as determined by the electroencephalographer are depicted at the bottom of the graph (the detection of the spindle in one channel was sufficient). IC5 and IC3 were visually settled as the ICs with the strongest spindles evidence. 12 ICs computed by extended *infomax* are depicted in Fig.8. The IC8 and IC4 were settled as the 'spindle' ICs.

The results of classification for all 7min recording are presented in Table 1. The number of spindles detected by electroencephalographer was 95. The total number of detected spindles is shown in the first column. The number of cases in which spindle was detected more than once is in the last column of the table. Classifications using different values of TC (number in brackets) for the strongest 'spindle' and the results using combination of two ICs with different TC are presented.

In Fig.9 the distribution of detected spindles over a scalp electrodes during the selected 50sec interval is depicted. The topographical mapping of the strength of the ICs computed over this interval is in Fig.10. In the next two figures (Fig.11 and Fig.12) the mapping of the ICs computed on first and second 25sec segments are presented. The 'spindle' IC were marked by stars. From visual observation we can hypothesize that there is a 'slight' correlation between the topographical projections of the ICs and distribution of the spindles over a scalp electrodes during a shorter time sequences (25sec). In spite of impossibility to determine the exact spatial distribution of the spindles sources we can hypothesize about

[3] http://www.cnl.salk.edu/~tewon/ica_cnl.html

	# of detections	# of correct	# of false negat.	# of false posit.	# of overlaps
EEG	121	91	4	30	3
fixed-point					
IC5 (0.02)	80	71	24	9	1
IC5 (0.01)	102	76	19	26	2
IC5 (0.02) + IC3 (0.04)	87	76	19	11	1
ext. *infomax*					
IC8 (0.02)	83	67	28	16	6
IC8 (0.01)	109	77	18	32	5
IC8 (0.02) + IC4 (0.04)	101	78	17	23	9

Table 1: Numbers of total detected, correct, false negative, false positive and overlapped cases of sleep spindle classification: comparison of using raw EEG data and 'spindle' ICs data. Values in brackets correspond to selected threshold constant (TC).

the frontal, central or occipital localization. We can observe similar results based on data from different 50sec data interval (Fig. 13-16).

6 Discussion

The experiments on simulated data confirmed the theoretical possibility of ICA method to separate a signal containing sleep spindles. The results obtained on real EEG data showed that ICA can partly separate the spindle activity into one IC. Using longer data intervals (in our case 7min EEG) two 'spindle' ICs were detected. In this case one 'spindle' IC was dominant in the sense that stronger evidence of sleep spindles was visually observed. There are usually 2-3 'spindle' ICs using shorter time sequences (25sec). Visual determination of dominant 'spindle' IC is not so easy as in former case [4].

The delays between occurrence of the spindles in different EEG channels complicate the classification algorithm proposed in [13]. The simple classification technique used for raw EEG data in our research led to a high number of spindle detections and thus to a high number of false positive classifications and to unsuitable overlap detections. Using 'spindle' IC for detection showed a high percentage of false negative classification. Smaller TCs decrease number of false negative classification at the expose of false positive classification. Using two ICs with different TC improved overall classification. We think that the big advantage of ICA to separate sleep spindle activity into 1 or 2 ICs should be expressed by proposing better classification algorithm in future. Using *fixed-point* algorithm led to slightly better classification results, however, better comparison have to be done here.

In [15] two different type of sleep spindles were detected and thus the hypothesis about two different spindle sources arose. Regarding to this, the question to separate spindle activity into one channel remains open.

The first investigations of possibility to detect the EEG electrodes containing spindles and thus partly determine the brain areas producing spindle activity are challenging but more investigations have to be done here. Especially in the cases where the 'spindles areas' change very quickly and thus we are constraint with convergence property of ICA.

In future work, we will investigate the possibility of using an extension of ICA for problems with time-delayed convolved sources. We hypothesize that this could lead to more exact evidence and location of the spindles in 'spindle' IC.

[4] We have to note, that in several cases of shorter time sequence one dominant 'spindle' IC was detected.

7 Acknowledgements

The authors thanks Prof. Zeitlhofer for providing EEG data set which was recorded at the Clinic of Neurology at the University of Vienna. This work was done as part of the Biomed-2 project BMH4-CT97-2040 SIESTA, sponsored by the EU Commission. The Austrian Research Institute for Artificial Intelligence is supported by the Austrian Federal Ministry of Science and Transport. The first author was partially supported by Slovak Grant Agency for Science (grants No. 2/5088/98 and No. 98/5305/468) and by scholarship provided by Action Austria-Slovakia.

References

[1] S. Amari, A. Cichocki, and H. H. Yang. A New Learning Algorithm for Blind Signal Separation. In D. Touretzky, M. Mozer, and M. Hasselmo, editor, *Advances in Neural Information Processing Systems 8*, pages 752–763. MIT Press, Cambridge MA, 1996.

[2] A. J. Bell and T. J. Sejnowski. An information maximisation approach to blind separation and blind deconvolution. *Neural Computation*, 7(6):1129–1159, 1995.

[3] J.F. Cardoso and B. Laheld. Equivariant adaptive source separation. *IEEE Transaction on Signal Processing*, 45(2):434–444, 1996.

[4] M. Girolami. *Self-organizing artificial neural networks for signal separation.* PhD thesis, Paisley University,Scotland, Department of Computing and Information Systems, 1997.

[5] A. Hyvärinen. Independent Component Analysis by Minimization of Mutual Information. Technical Report A46, Helsinki University of Technology, Laboratory of Computer and Information Science, August 1997.

[6] A. Hyvärinen and E. Oja. A Fast Fixed-Point Algorithm for Independent Component Analysis. *Neural Computation*, 9:1483–1492, 1997.

[7] T.P Jung, C. Humphries, T. W. Lee, S. Makeig, M. J. McKeown, V. Iragui, and T. J. Sejnowski. Extended ICA removes artifacts from electroencephalographic recordings. In *Advances in Neural Information Processing Systems 10.* MIT Press, 1998.

[8] T.W. Lee, M. Girolami, A.J. Bell, and T.J. Sejnowski. A unifying Information-theoretic framework for Independent Component Analysis. *International Journal on Mathematical and Computer Modeling*, 1998. in press.

[9] T.W. Lee, M. Girolami, and T.J. Sejnowski. Independent Component Analysis using an Extended Infomax Algorithm for Mixed Sub-Gaussian and Super-Gaussian Sources. *Neural Computation, in press*, 1998.

[10] S. Makeig, T. P. Jung, A. J. Bell, D. Ghahremani, and T. J. Sejnowski. Blind separation of auditory event-related brain responses into independent components. In *Proceedings of the National Academy of Sciences*, number 94, pages 10979–10984, 1997.

[11] J.P. Nadal and N. Parga. Non-linear neurons in the low-noise limit: a factorial code maximises information transfer. *Network*, 4:295–312, 1994.

[12] A. Rechtschaffen and A. Kales. A manual of standardized terminology technique and scoring system for sleep stages of human subject. Technical report, University of California, 1968.

[13] P. Schimicek, J. Zeitlhofer, P. Anderer, and B. Saletu. Automatic Sleep-spindle Detection Procedure: Aspects of Reliability and Validity. *Clinical Electroencephalography*, 25(1):26–29, 1994.

[14] R. Vigário. Extraction of ocular artifacts from EEG using independent component analysis. *Electroencephalography and clinical Neurophysiology*, 103:395–404, 1997.

[15] E. Werth, P. Achermann, D. J. Dijk, and A. A. Borbély. Spindle frequency activity in the sleep EEG: individual differences and topographic distribution. *Electroencephalography and clinical Neurophysiology*, 103:535–542, 1997.

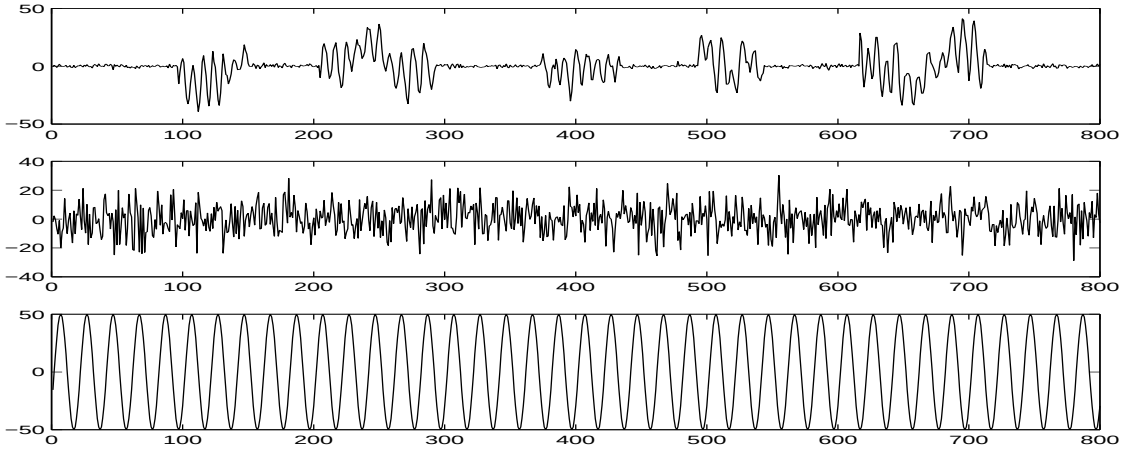

Figure 1: The source signals. Sleep spindles signal (s_1), white noise with Gaussian distribution (s_2) and periodic signal (s_3). Estimated kurtosis: $k(s_1) = 6.661, k(s_2) = 0.031, k(s_3) = -1.5$.

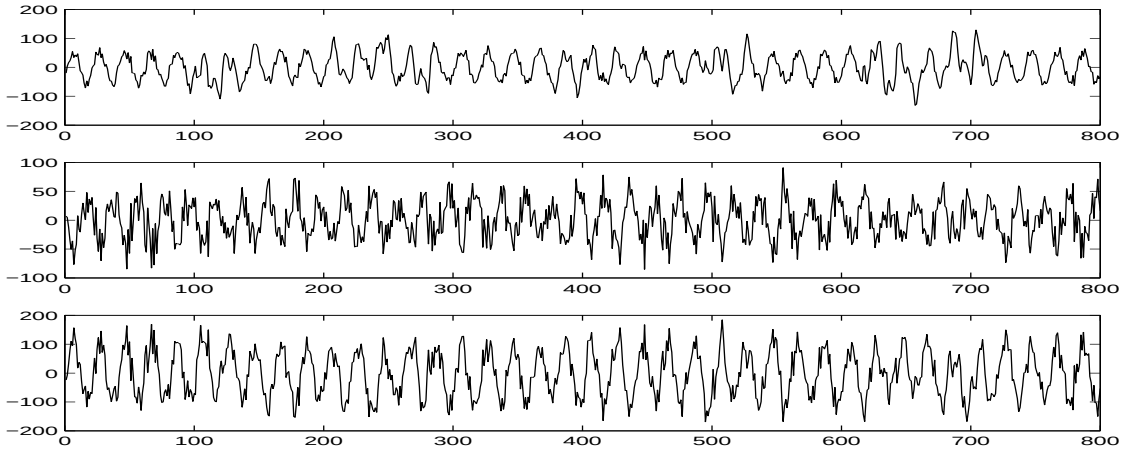

Figure 2: Mixed signals x_1, x_2, x_3. Estimated kurtosis: $k(x_1) = 0.622, k(x_2) = -0.553, k(x_3) = -0.735$.

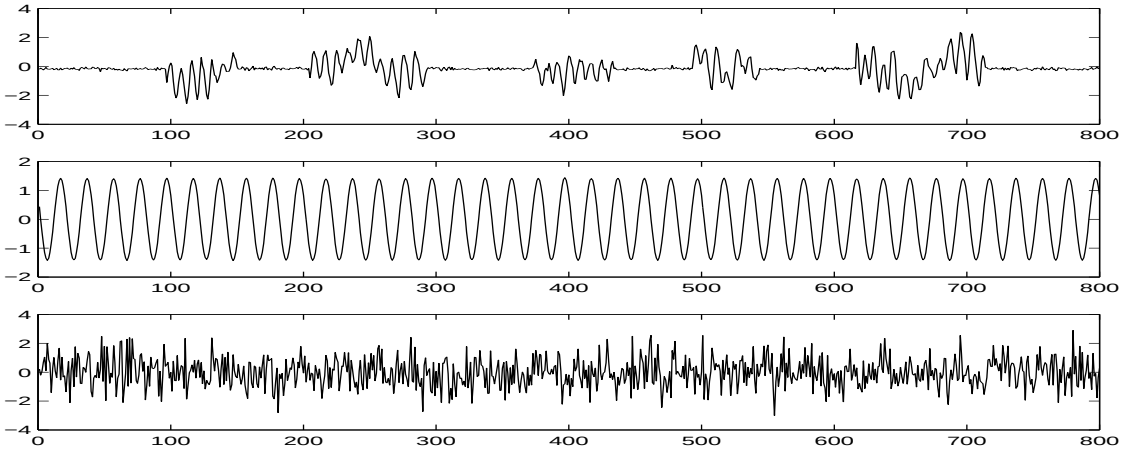

Figure 3: Estimated source signals u_1, u_2, u_3 using *fixed-point* algorithm. Estimated kurtosis: $k(u_1) = 6.667, k(u_2) = -1.5, k(u_3) = 0.032$.

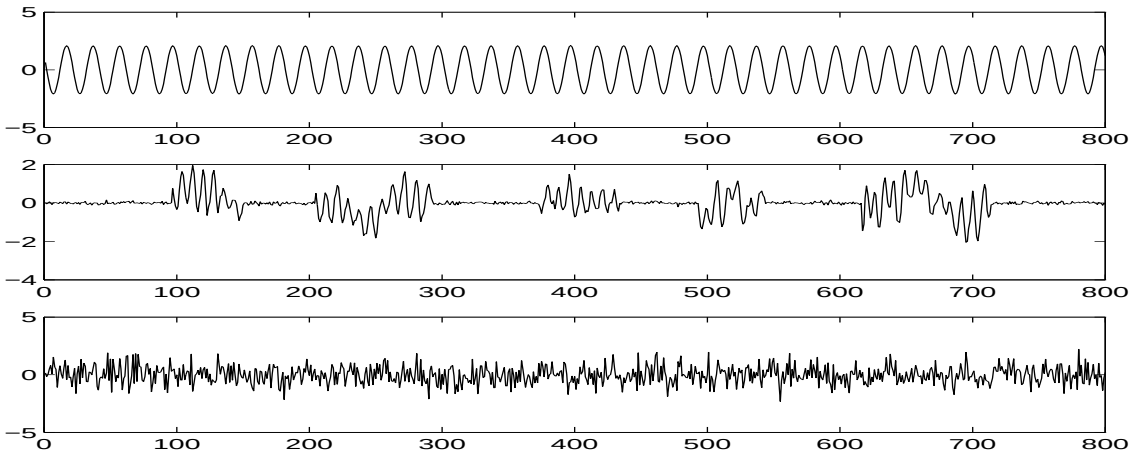

Figure 4: Estimated source signals y_1, y_2, y_3 using extended *infomax* algorithm. Estimated kurtosis: $k(y_1) = -1.5, k(y_2) = -6.668, k(y_3) = 0.032$.

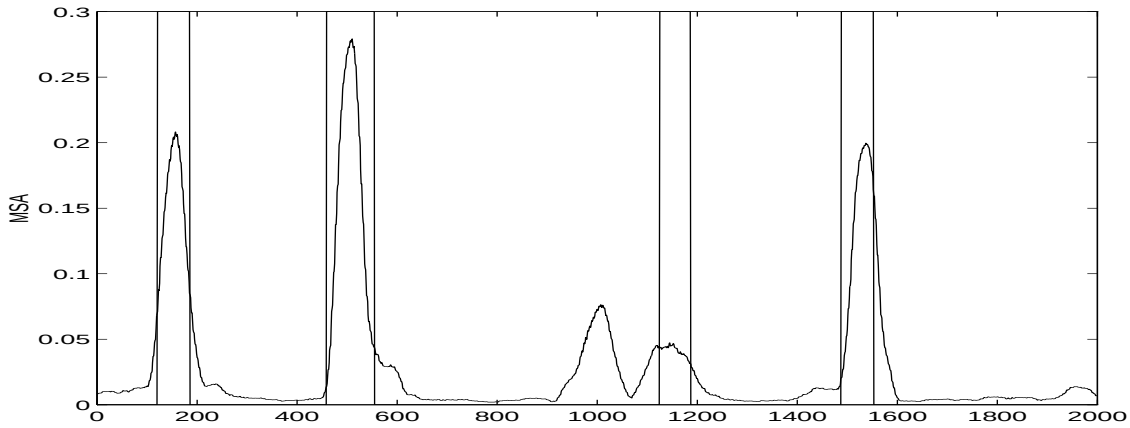

Figure 5: An example of impossibility to determine a unique threshold constant (TC) correct for all sleep-spindles determined by electroencephalographer (intervals between vertical lines). The TC suitable to detect a third 'correct' spindle will lead to one false positive detection ('bump' centered around value 1000).

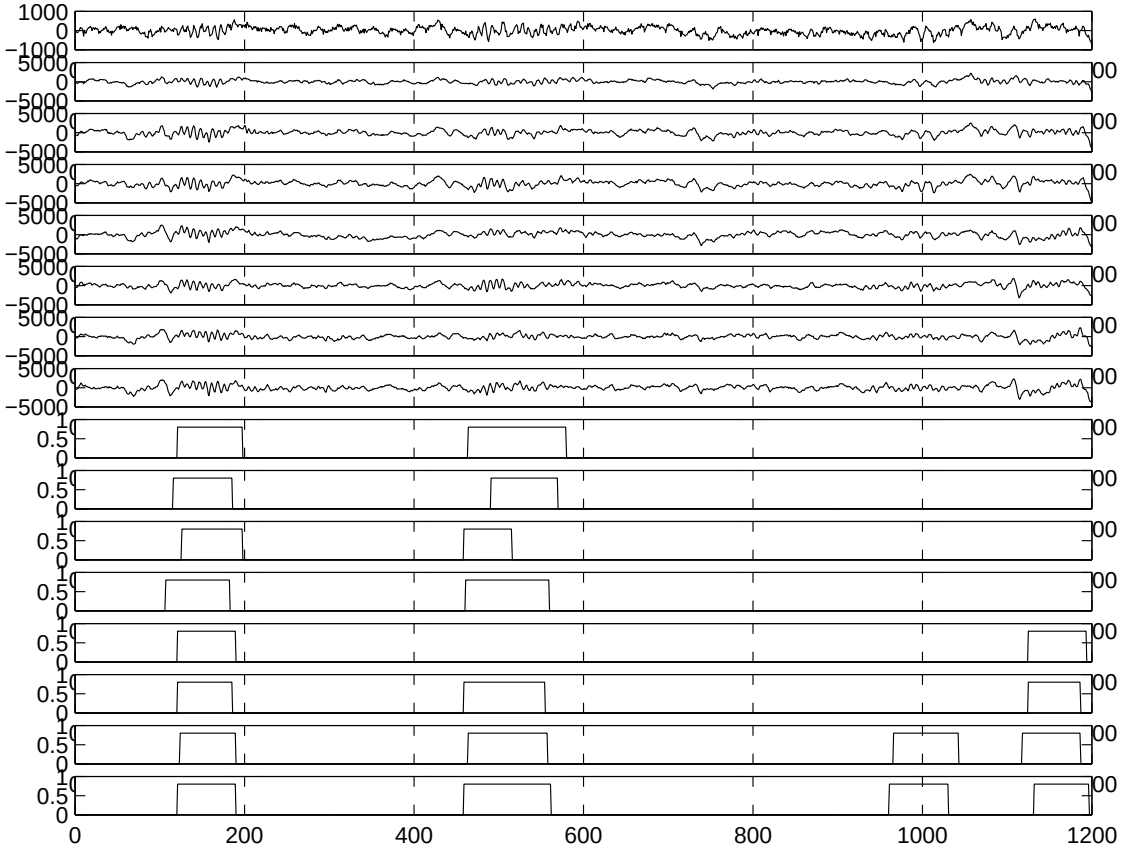

Figure 6: 12sec recording of 8 EEG channels (Fp1, F8, F4, Fz, C4, C3, P4, Pz) with sleep spindles marks determined by electroencephalographer.

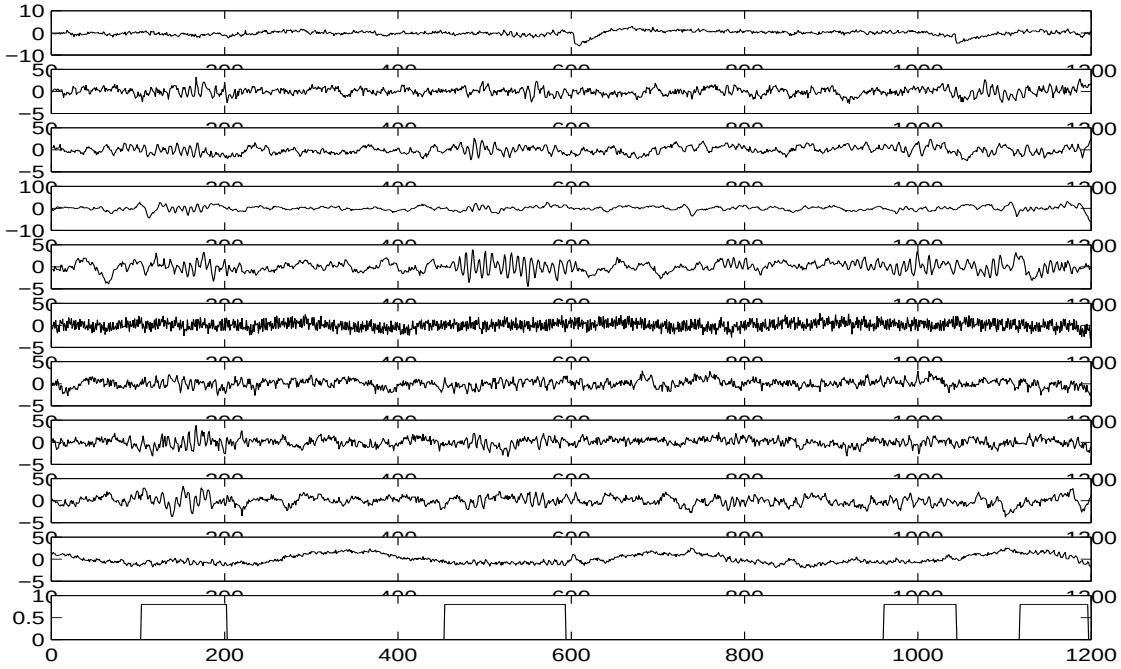

Figure 7: First 10 ICs computed by *fixed-point* algorithm (time aligned with Fig.6) with sleep spindles marks determined by electroencephalographer.

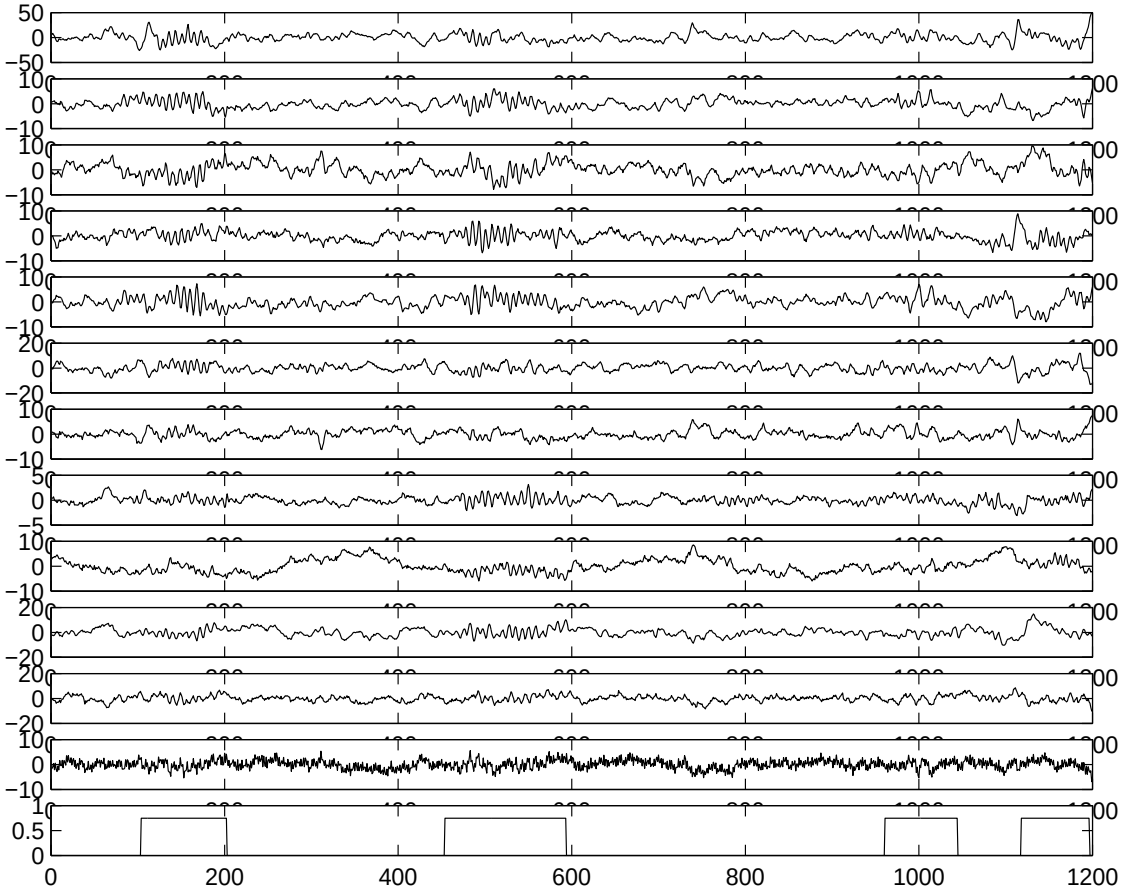

Figure 8: 12 ICs computed by extended *infomax* algorithm (time aligned with Fig.6) with sleep spindles marks determined by electroencephalographer.

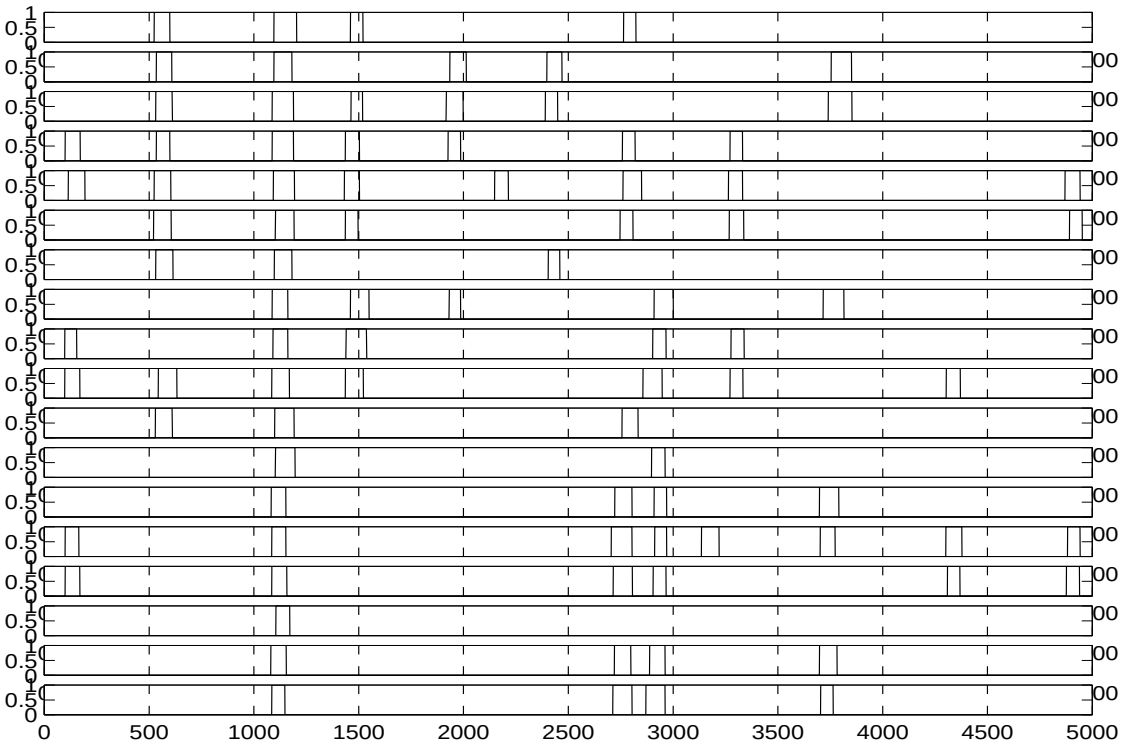

Figure 9: Marks of the spindles detected by eletroencephalograhper during the 50sec data interval. Order of the channels from top to bottom: Fp1,F8,F4,Fz,F3,F7,T4,C4,Cz,C3,T3,T6,P4,Pz,P3,T5,O1,O2.

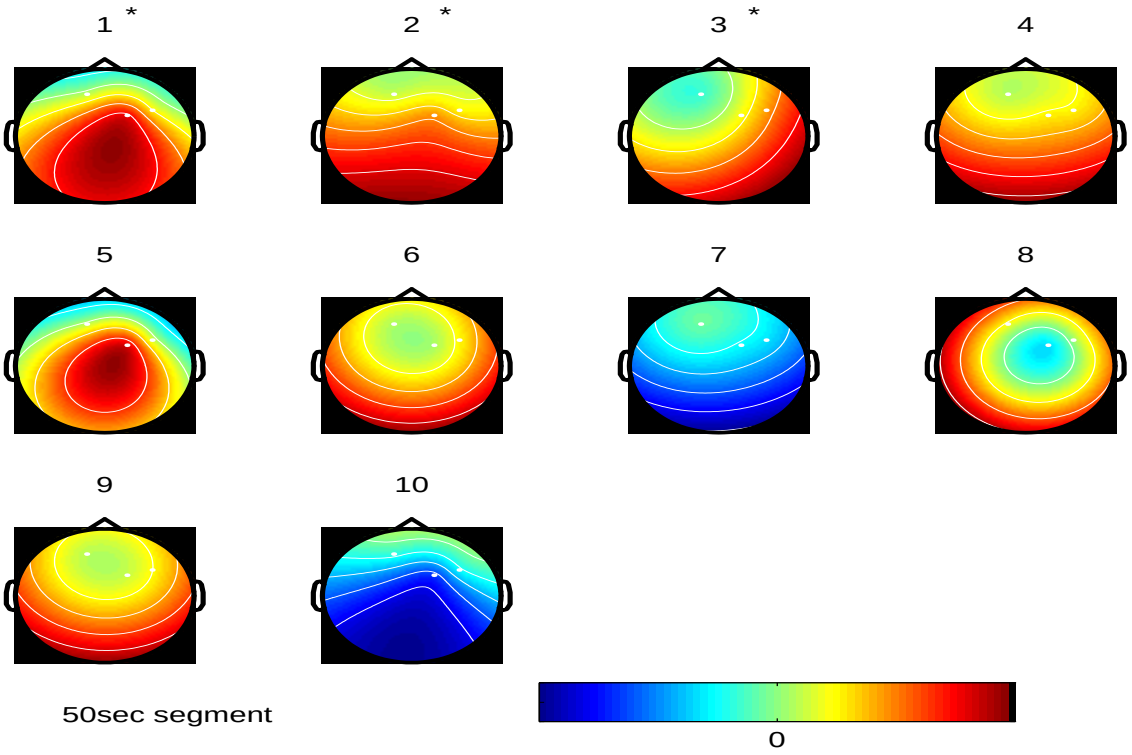

Figure 10: Projection of the ICs computed from 50sec data interval (Fig.10) onto the scalp sensors.

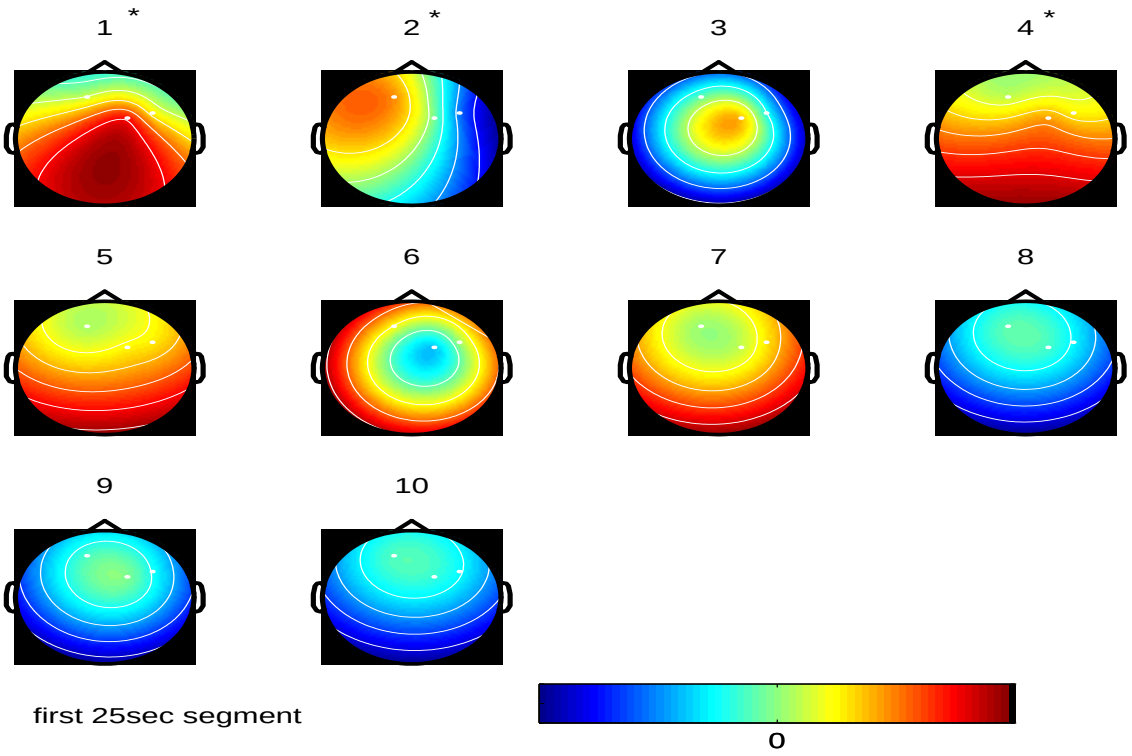

Figure 11: Projection of the ICs computed from first 25sec data interval (Fig.10) onto the scalp sensors.

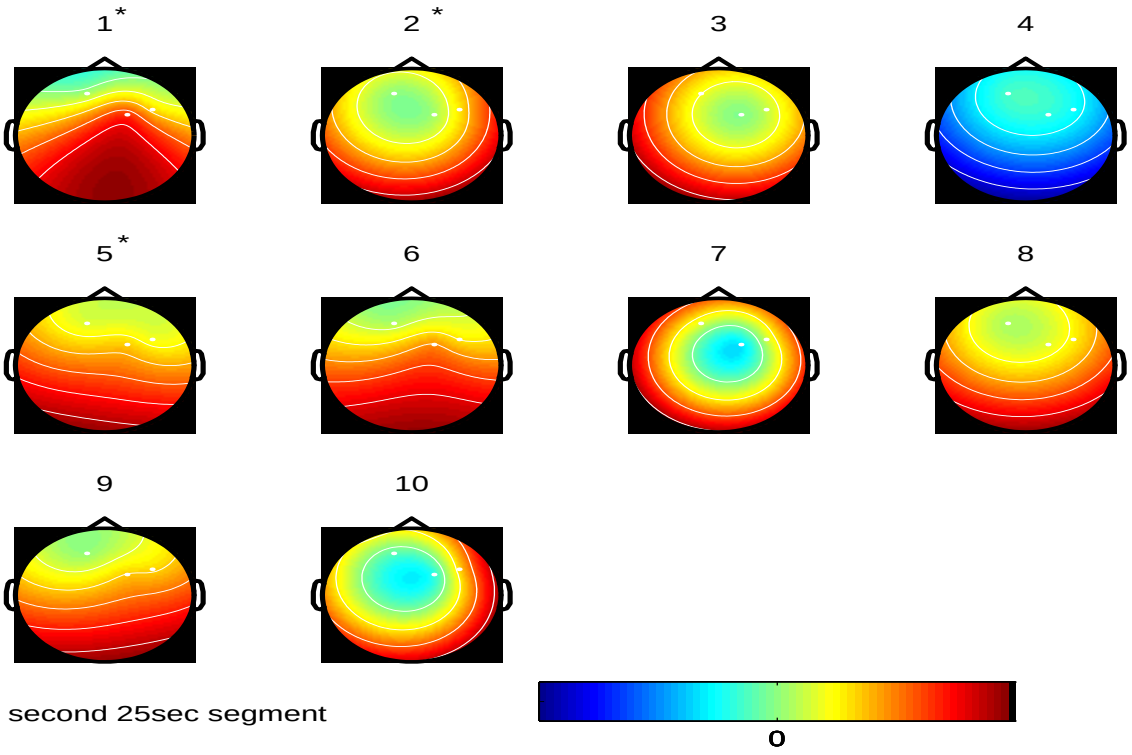

Figure 12: Projection of the ICs computed from second 25sec data interval (Fig.10) onto the scalp sensors.

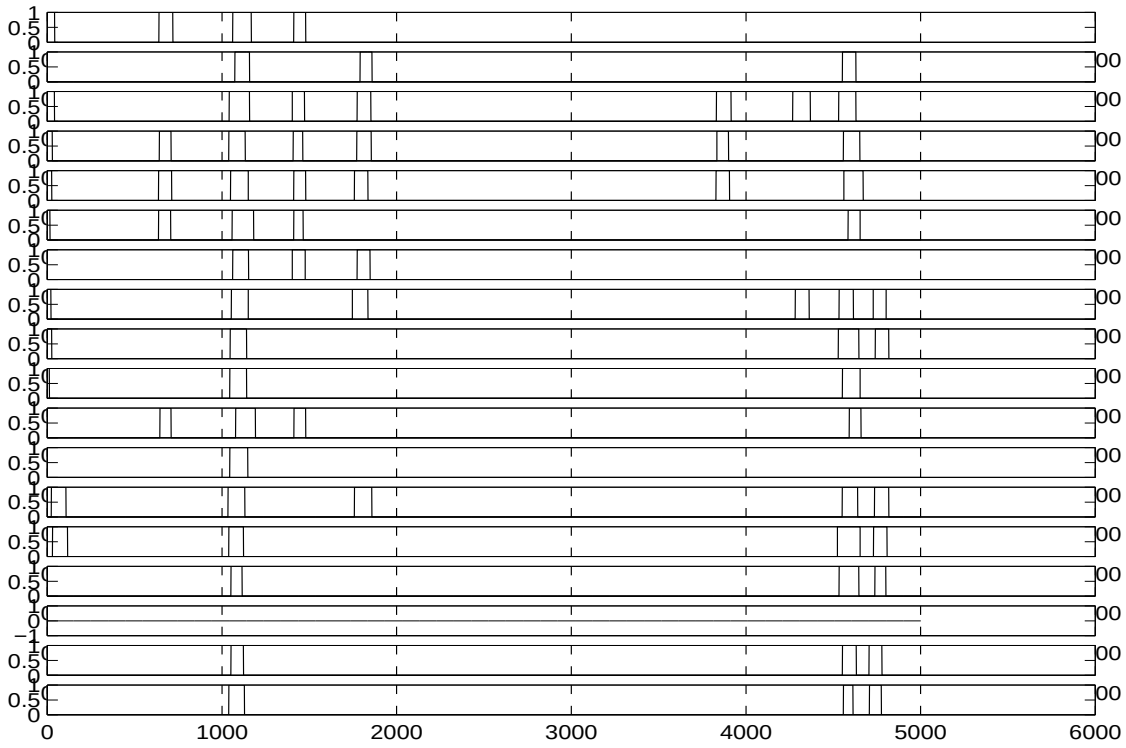

Figure 13: Marks of the spindles detected by eletroencephalograhper during the 50sec data interval. Order of the channels from top to bottom: Fp1,F8,F4,Fz,F3,F7,T4,C4,Cz,C3,T3,T6,P4,Pz,P3,T5,O1,O2.

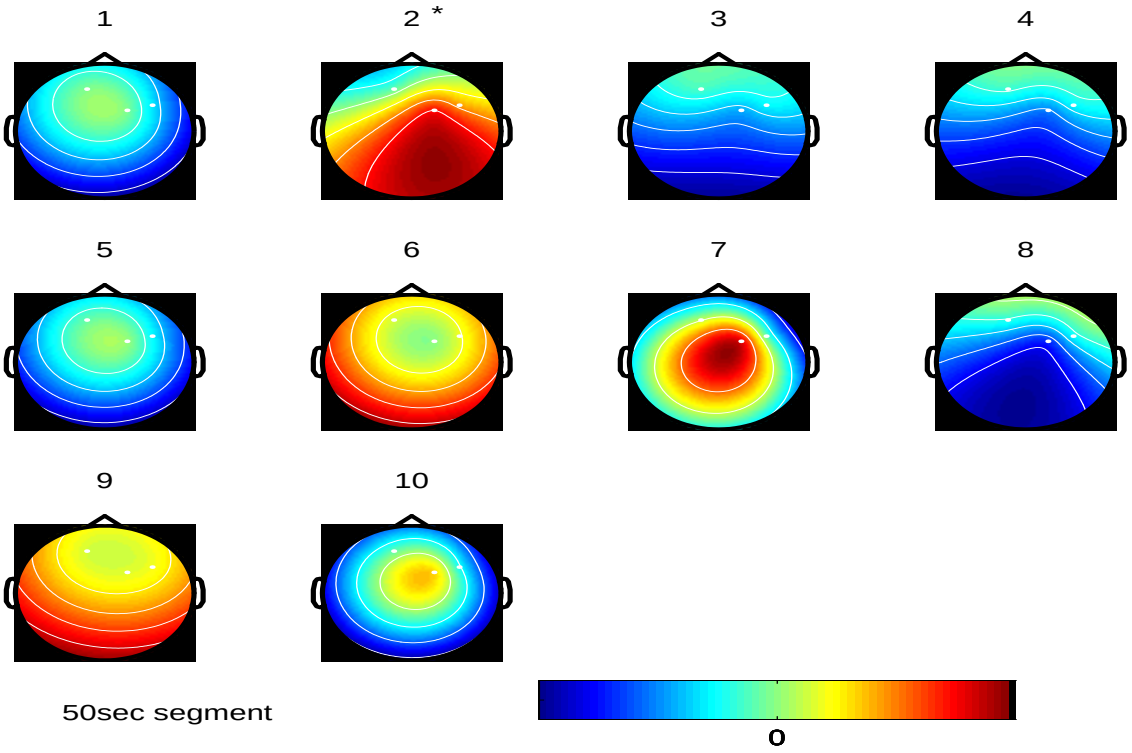

Figure 14: Projection of the ICs computed from 50sec data interval (Fig.10) onto the scalp sensors.

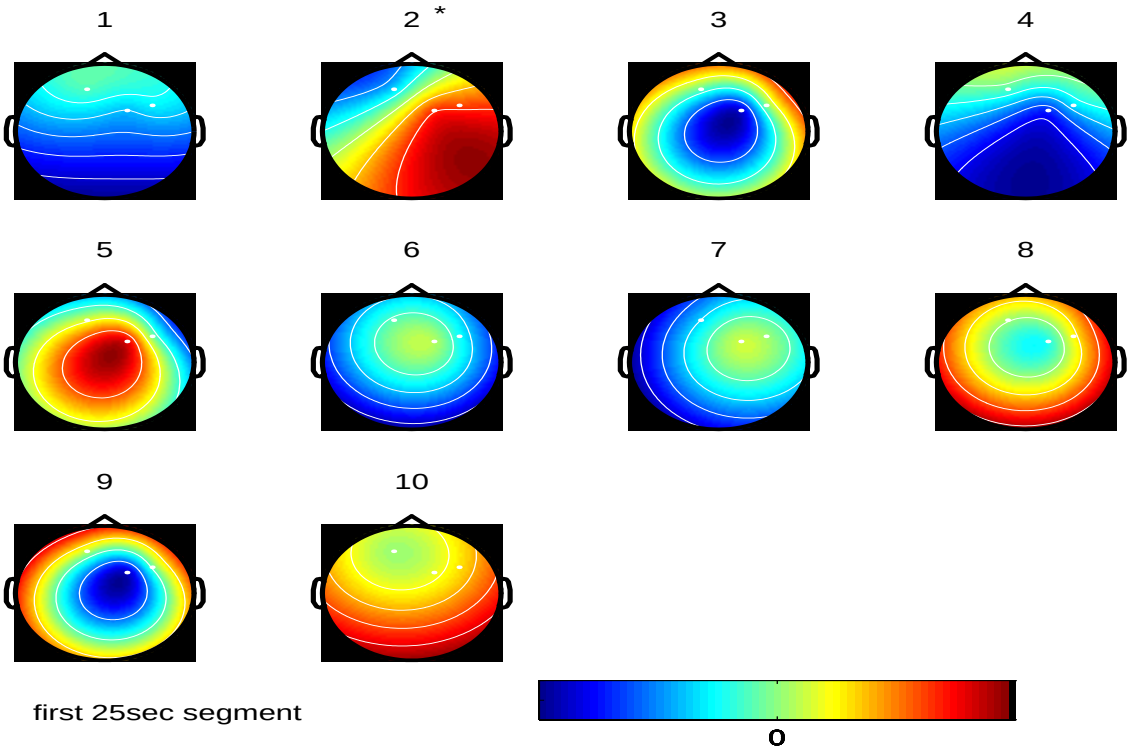

Figure 15: Projection of the ICs computed from first 25sec data interval (Fig. 10) onto the scalp sensors.

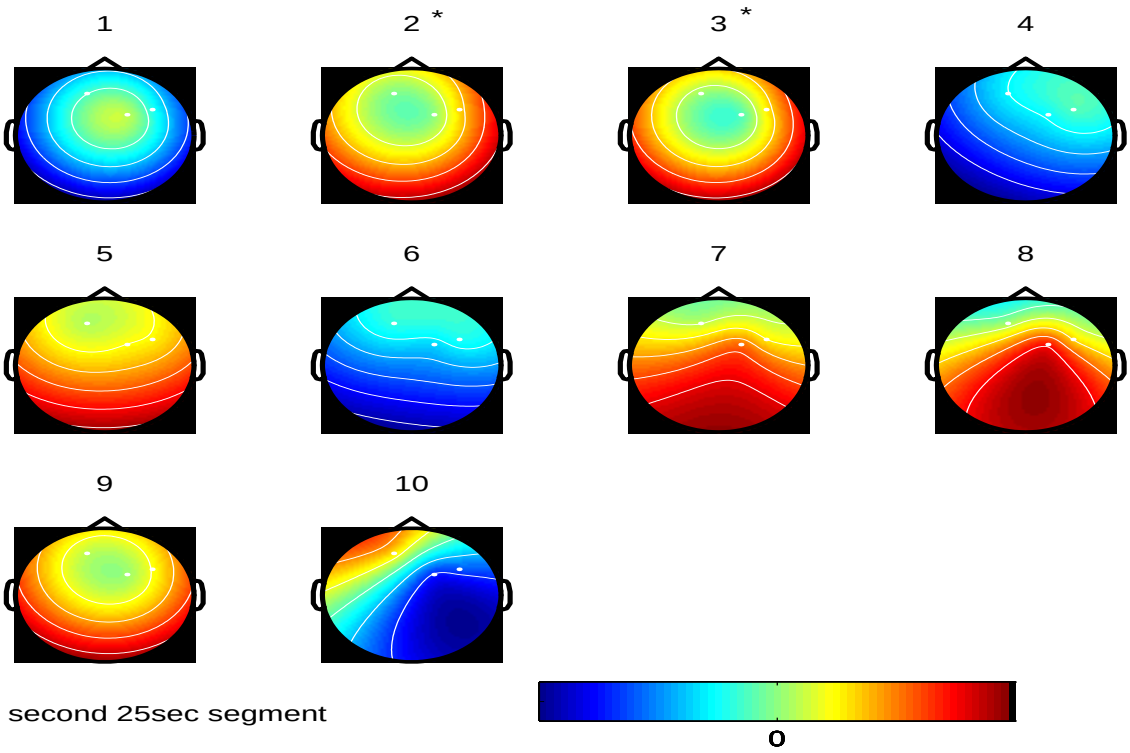

Figure 16: Projection of the ICs computed from second 25sec data interval (Fig.10) onto the scalp sensors.